Construction and Building Materials 275 (2021) 122159
https://doi.org/10.1016/j.conbuildmat.2020.122159

Constitutive modelling and mechanical properties of cementitious composites incorporating recycled vinyl banner plastics

D.V. Bompa[1,2*], B. Xu[3], A.Y. Elghazouli[2]

Department of Civil and Environmental Engineering, University of Surrey, Guildford, GU2 7XH, UK
Department of Civil and Environmental Engineering, Imperial College London, SW7 2AZ, UK
Xi'an Jiaotong-Liverpool University, Department of Civil Engineering, Suzhou, 215123, China.

Abstract

This paper describes an experimental study, which has been lacking to date, into the mechanical properties of cementitious composites incorporating granules and fibres from recycled Reinforced PVC (RPVC) banners. A detailed account of more than 140 tests on cylindrical, cubic and prismatic samples tested in compression and flexure, with up to 20% replacement of mineral aggregates, is given. Based on the test results, the uniaxial properties of selected recycled materials are examined in conjunction with a detailed characterisation of the RPVC granule size and geometry. Experimental measurements using digital image correlation techniques enable a detailed interpretation of the full constitutive response in terms of compression stress-strain behaviour and flexural stress-crack opening curves, as well as key mechanical parameters such as strength, elastic modulus and fracture energy. It is shown that the mechanical properties decrease proportionally with the amount of RPVC. For each 10% increment of volumetric replacement of mineral aggregates, the compressive strength is halved whilst the flexural strength is reduced by about 30% compared to their conventional counterparts. The reduction in strength is counterbalanced by an improved ductility represented by a favourable post-peak response in compression and an enhanced flexural softening and post-cracking performance. Smaller particles, with a relatively long acicular or triangular geometry, exhibited better behaviour as these acted as fibres with improved bond properties in comparison with intermediate and large size granules. The test results and observations enable the definition of a series of expressions to determine the mechanical properties of cementitious materials incorporating RPVC and other waste plastics. These expressions are then used as a basis for an analytical model for assessing the compressive and tensile stress-strain response of such materials. Validations carried out against the tests carried out in this study, as well as from previous investigations, indicate that the proposed expressions and the developed constitutive model offer reliable representations for practical application.

Keywords: Plastic waste; Cementitious composites; Reinforced PVC; Recycling; Constitutive models.

**Corresponding author: Dr. D.V. Bompa*
Emails: D.V. Bompa (d.bompa@surrey.ac.uk), B. Xu (bowen.xu@xjtlu.edu.cn), A.Y. Elghazouli (a.elghazouli@imperial.ac.uk),

1. Introduction

The versatility and applicability of polymers have permitted the development of a wide range of plastic materials. Over the past half-century, the use and importance of such materials in consumer and industrial applications have continuously grown, with the global plastic production reaching over 300 million tonnes per year, and this is expected to double within the next two decades [1]. The ever-growing plastic production poses significant environmental and health effects. Large quantities of plastics are discarded in landfills or incinerated (31-39%), or reach the oceans (1.5-4%), whilst only a small proportion is collected for recycling in Europe (<30%). Recent international strategies have therefore been adopted to curb plastic waste and littering as well as the amount of recycled plastics.

Polyvinyl chloride (PVC) accounts for the fifth and third-largest categories of plastics produced in the world and Europe, respectively [2]. It is employed in a wide range of applications in building and construction, packaging, and other industries. Vinyl materials are also used as polymer coated fabrics in advertising banners, lorry covers and flags. Due to the short-term use of RPVC banners in advertising, they are typically discarded in landfill at the end of their life, with only a limited quantity, particularly large-size banners, being reused as tent components for emergency sheltering. The main challenges posed to end-of-life banner recycling is the intrinsic nature of the constituent elements which are a mixed vinyl film-polyester scrim material provided with grommets placed all along the hem for tie-off points. Unsurprisingly, in the UK, coated fabrics represent only 1.4% of the total PVC recycled and a very small proportion is upcycled in clothing and leisure elements [3].

As for many waste materials, typical recycling routes for PVC are mechanical, chemical or energy recovery. Energy recovery is associated with the release of toxic fumes and carbon dioxide into the atmosphere, and produces solid residues such as slag or ash [3-5]. On the other hand, chemical recovery is based on material degradation, whilst mechanical recovery involves shredding or grinding in chips or powder [7,8]. Although several strategies are in place for plastic recycling, limited studies have been undertaken on the recycling or reuse of end-of-life banners. For example, an investigation which is based on mechanical recovery involves shredding of end-of-life banners along with recycled cables [9]. These are mixed together and further employed as a base material for plastic manufacturing techniques.

A number of previous investigations have focused on the performance of mortars and concrete materials provided with recycled particles as aggregates, fillers or fibres [10-13]. Waste plastics typically used in concrete include Polyethylene Terephthalate (PET) [14-17], High-Density Polyethylene (HDPE) [19,20], Low-Density Polyethylene (LDPE) [21,22], Poly Vinyl Chloride

(PVC) [13, 23, 24], Polypropylene (PP) [25-27] or Polystyrene [28] elements in the form of granules, chips, shreds or fibres. These are typically recovered from bottles, packaging, textiles, electronic parts or plastic bags.

When the waste plastics are used as aggregates, the proportion replaced influences the fresh, mechanical, physical and long-term properties of the composite in a proportional manner to the quantity and properties of the mineral aggregates replaced [16,17,29]. For example, 15% replacement improves the eco-efficiency and sustainability, yet it impairs its fresh state unless additives are used, and reduces the compressive strength to about 35% of its reference counterpart [27]. Moreover, in comparison to normal concrete, the concrete compressive strength decreases by 5%, 15% and 30%, with an increase of plastic content of 25%, 50% and 75%, respectively [15]. On the other hand, the use of waste plastics in concrete can improve its toughness as it leads to absorption of higher amounts of energy in comparison with conventional concrete materials [10].

Although various studies have been undertaken on incorporating waste plastics in cementitious mixes, there is a lack of investigations in general on the use of recycled elements from Reinforced PVC banners in construction materials, including those from end-of-life banners. In particular, assessments of the main mechanical parameters of materials incorporating aggregates resulting from recycling of waste plastics are limited [30]. To this end, this study examines the potential use of granules and fibres from recycled banners in cementitious mixes, with particular focus on the uniaxial properties of recycled RPVC materials and the influence of particle size and proportion on the mechanical properties of mortars and concrete composites. A set of design expressions to determine the main mechanical properties, including the elastic modulus, compressive, flexural and splitting strengths, as well as a complete constitutive model to assess the compressive and tensile stress-strain relationship of cementitious composites provided with plastic aggregates, are proposed.

2. Experimental programme

The influence of Reinforced PVC (RPVC) granules and fibres resulting from recycled banners on the mechanical properties of high strength mortars and concrete was examined through a set of 140 samples tested in compression and flexure, equally divided across a total of 13 mortar and 2 concrete mixes. Compression mortar tests were carried out on cylinders of Ø75 mm diameter and 150 mm length, and cubic samples of 50 mm side length. Three-point bending tests for flexural strength assessment were undertaken on plate samples with 25 mm depth, 55 mm width and 150 mm length. The parameters that were directly varied within the experimental programme were the volume of mineral aggregate replaced (2.5%, 5%, 10% and 20%, corresponding to a replacement

ratio of ρ_{vp}=0.025, 0.05, 0.1 and 0.2, respectively) as well as the plastic granule size d_p (small: 1.25 mm > d_p > 2.50 mm; intermediate: 2.50 mm > d_p > 5.0 mm; large: 5.0 mm > d_p > 10.0 mm). The specimen reference adopts the format TR-VV-FF, which indicate the sample type T (C for circular/cylinder, S for square/cube, B for rectangular/plate), composite material R (M for mortar and C for concrete), volume of mineral aggregate replaced (V) and size of the plastic granule (F).

For example, CM-10.0-1.25 represents a cylindrical sample made of mortar which has 10% replacement of mineral aggregates with small RPVC granules (1.25 mm > d_p > 2.50 mm). In addition to the mortar samples incorporating RPVC granules in the form of chips, a number of additional tests on high strength concrete Ø100×200 cylinders and 100×100×500 mm prisms were carried out. These incorporated RPVC fibres with l_f=70 mm length and w_f=3 mm width in a proportion of 0.5%. The specimen reference adopts the same format, but instead of the size of the granule the aspect ratio of the fibre is used as w_f/l_f=0.05 (e.g. CC-0.5-0.05). The 13 mortar mixes enable an in-depth understanding of the influence of incorporating various RPVC proportions and particle sizes on the mechanical properties of RPVC composites. On the other hand, the results from the high strength concrete tests contribute to identifying technological challenges occurring from adding fibre elements. Complementary uniaxial tests on selected RPVC materials have also been carried out as described below.

2.1 Reinforced PVC properties

To quantify the mechanical properties of the adopted RPVC materials, three types of banners obtained from a recycler were selected for uniaxial testing: (i) Type I - white coated fabrics with unidirectional reinforcement, (ii) Type II - bi-directional mesh with 0.5 mm hole size and (iii) Type III - red bi-directional reinforced fabrics. The measured thickness of the three types was 0.3 mm, 0.35 mm and 0.52 mm, respectively. Three specimens of 250 mm length and 25 mm width were prepared for each material group. These were provided with 50 mm tabs at both ends to ensure adequate griping in the testing machine. The clear length between testing jaws was l_s=150 mm. A uniaxial Instron testing machine with a maximum capacity of 150 kN was used to test the specimens under monotonically increasing displacement with a displacement rate of 0.1 mm/min. To assess the strength and deformation characteristics, the load and displacement recorded by the machine were divided by the coupon area and by the clear length, respectively.

As indicated in Figure 1, all materials exhibited a largely elastic stress-strain behaviour up to failure. Type I materials had a relatively low strength with an average ultimate strength f_f=26.0 MPa. Type II was about three times stronger reaching f_f=129.0 MPa, whilst Type III failed at an average f_f=80.8 MPa. The latter is a relatively strong element with tensile strength about 25% of

reinforcement steels and about 50% of structural steels typically used in construction. The minimum ultimate deformation was 11%, 30% and 26% for Type I, II and III, respectively.

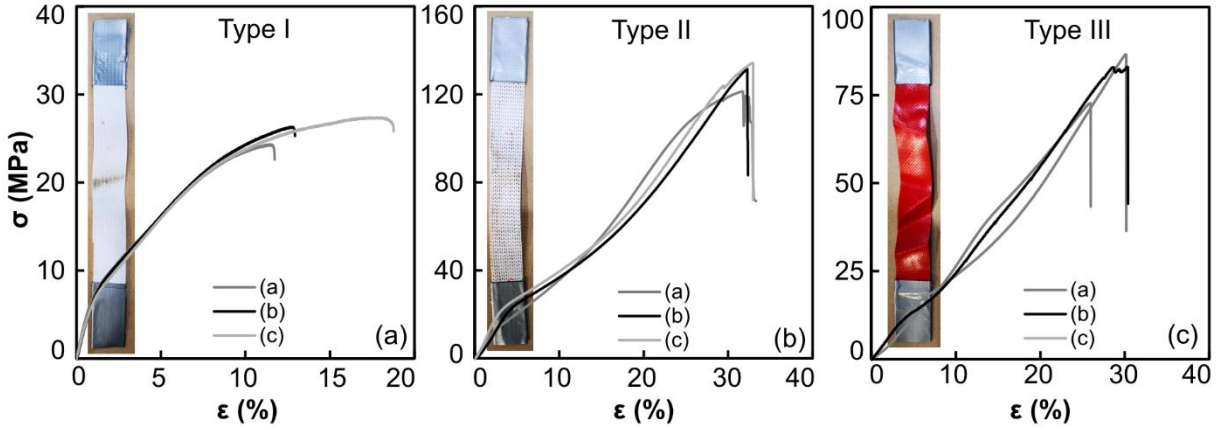


Figure 1 Uniaxial properties of selected recycled banner materials: a) Type I – white; b) Type II -mesh; c) Type III - red

These results indicate that Type II and III could be incorporated in concrete elements as strips/fibre for structural applications to enhance the flexural ductility and fatigue strength, whilst Type I could be used only in low-grade elements such as pavements. To minimise costs related to sorting the recycled banners, a blend of mixed recycled banners were chosen for shredding and were sieved using a standard aggregate sieve in the following particle sizes: (i) small - 1.25 mm > d_p > 2.50 mm, (ii) intermediate - 2.50mm > d_p > 5.0 mm, and (iii) large - 5.0 mm > dp > 10.0 mm (EN 933-1 [31]). Additionally, Type III materials were selected to be incorporated in concrete as fibres with 70 mm length and 3 mm width in a proportion of 0.5%, as mentioned before.

The shredded granules were sieved using a standard aggregates sieve in three sizes and were used in the condition received from the recycler without pre-treatment. As shown in Figure 2, the granules had polygonal shapes with non-uniform geometries and relatively random distribution. To characterise the granule size as well as their distribution, an arbitrary sample of 50g of material for each sieved granule size was selected and spread on a white sheet (see right-hand panels of Figures 3a,b,c). Images taken with a high-resolution camera were then processed using an open-source software by removing colours and enhancing contrast, to facilitate detection of particle boundaries. The particle size distribution within the arbitrary sample was determined using image processing algorithms from binary 2d images [32].

Figure 3 depicts the relationship between the frequency ratio of granule occurrence within the arbitrary 50g sample (f/N) and the equivalent particle radius ($r_{p,eq}$). It is shown that the average particle radius is $r_{p,avg}$=1.39 mm for particles passing through '1.25 mm > d_p > 2.50 mm' sieve; $r_{p,avg}$=2.16 mm for particles passing through 2.50 mm to 5.0 mm sieve; and $r_{p,avg}$=4.12 mm for particles passing sieve gaps greater than 5.0 mm but less than 10 mm.

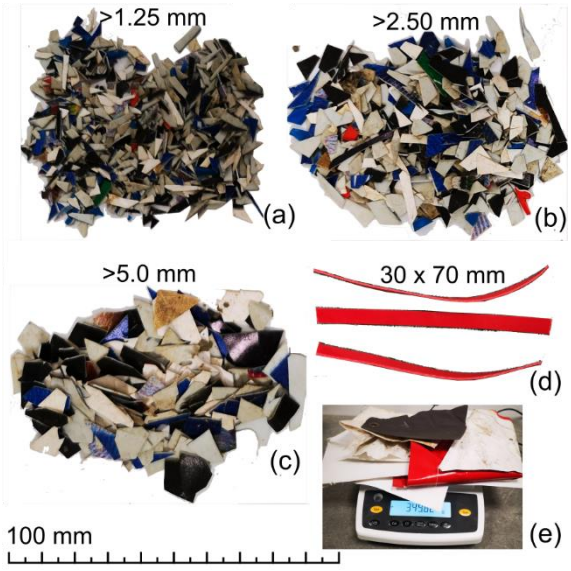


Figure 2 Size and shape of processed recycled RPVC banners: granules with: a) 1.25 mm > d_p > 2.50 mm, b) 2.50mm > d_p > 5.0 mm, c) 5.0 mm > dp > 10.0 mm; d) macrofibres of 30 × 70 mm; e) Unprocessed RPVC banners

As observed, the average diameter of the particle group with the smallest size $d_{p,avg}$=2.78 mm is above the upper bound of the sieve gap (1.25 mm to 2.50 mm). In contrast, the intermediate and large size particles with $d_{p,avg}$=4.32 mm and $d_{p,avg}$=8.24 mm, respectively, are within the sieve limits. This confirms that most of the small size particles are relatively long and have a triangular or acicular geometry that passes the 2.50 mm sieve although their average diameter is 2.78 mm. This RPVC granule size characterisation helps provide an insight into the compatibility between mineral aggregates and those from recycled materials, and also enables a detailed interpretation of the relationship between mechanical properties of RPVC mortars and concrete with respect to RPVC size and characteristics.

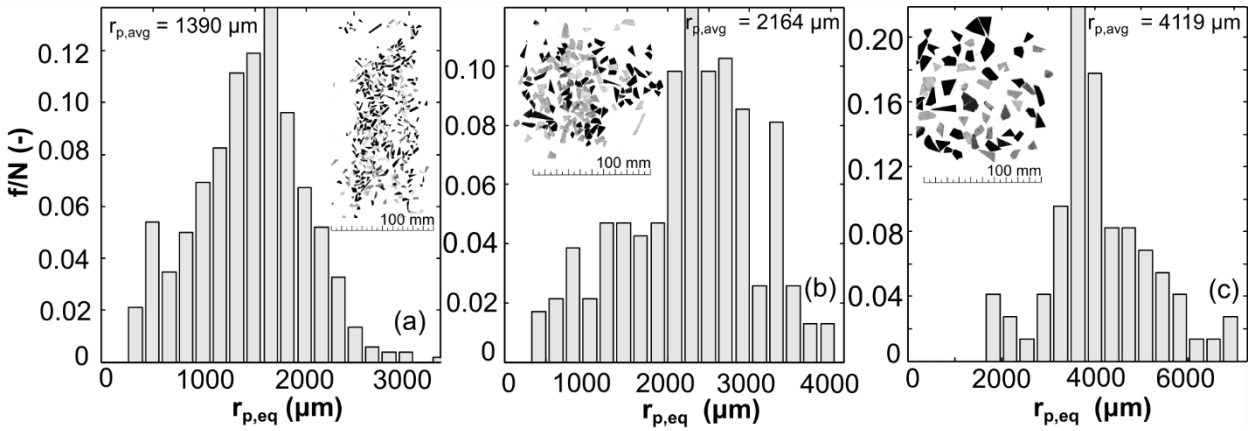


Figure 3 Granule size distribution for granules with: a) 1.25 mm > d_p > 2.50 mm, b) 2.50mm > d_p > 5.0 mm, c) 5.0 mm > dp > 10.0 mm;

2.2 Mixes and samples

As mentioned before, 13 mortar mixes and 2 concrete mixes incorporating recycled RPVC particles were prepared. Mortar mixes included cement, fly ash, microsilica, RPVC granules, fine mineral aggregates, tap water and admixtures, whilst in the concrete mixes, coarse mineral aggregates were also present (Table 1). CEM I 52.5 cement was used as the primary binder (EN-197-1 [33]). Secondary binders, which replace 50% of the cement from the reference mix, were EN 450-1 fineness category S fly ash (EN 450-1 [34]) and undensified Grade 940 microsilica with a minimum of 90% SiO2. These represented 35% and 15% of the total binder content, respectively. Also, polycarboxylate superplasticizer admixtures were added to improve the workability of the mixes. The fine mineral aggregates used in the mortar mixes had a particle size < 5 mm, a specific gravity of 2.65 and a fineness modulus of 2.35. In addition to these particles, the concrete mixes had coarse aggregates (5-10 mm) with a specific gravity of 2.65 and a fineness modulus of 5.88. These materials were used to produce a set of 117 mortar and 24 concrete test samples.

Table 1 Mix details

Constituent	M-0-0	M-2.5-*	M-5-*	M-10-*	M-20-*	C-0-0	C-0.5-0.05
CEM I (kg/m^3)	230	230	230	230	230	230	230
Fly Ash (kg/m^3)	161	161	161	161	161	161	161
Microsilica (kg/m^3)	69.0	69.0	69.0	69.0	69.0	69.0	69.0
RPVC	-	23.0	46.0	93.0	186	-	5.0
Sand (0-5mm) (kg/m^3)	1734	1690	1647	1560	1387	687	687
Gravel (5-10mm) (kg/m^3)	-	-	-	-	-	1145	1145
Water (l/m^3)	152	152	152	152	152	152	152
Admixtures (l/m^3)	9.2	9.2	9.2	9.2	9.2	9.5	9.5

* stands for different plastic granule sizes (d_p): a – 0.625 mm > d_p > 1.25 mm >; b – 1.25 mm > d_p > 2.50 mm; c - 2.50 mm > dp > 5.0 mm;

The mixing procedure from EN 1015-2 [35] was followed to produce mortars from dry constituents, water and admixtures. It is worth noting that a relatively low water-to-binder (w/b) ratio was initially considered. However, to reach a flow value representative of workable mortars, this was adjusted to a value of around 0.33. A mortar mix with a homogenous dispersion of RPVC granules for all particle sizes was obtained with this (w/b) ratio. The consistency of fresh mortar, assessed by means of a flow table, was above 130 mm. The concrete materials also had very good workability and required a minimum level of compaction. However, due to the intrinsic flexibility of the RPVC fibres combined with the relatively high length/width aspect ratio, the fibre dispersion was relatively non-homogeneous and some fibres, around 10%, remained stuck to the mixing paddle.

These issues are related to the influence of the fibre content, fibre aspect ratio, fibre stiffness and mixing procedure.

All mortars were prepared in 7-litre batches using a rotary mixer with a 20-litre capacity, whilst the concrete was prepared in batches of 24-litres in a 40-litre mixer. The dry constituents were mixed for a period of 180s, followed by the gradual addition of water, then mixed for another 180s. For each of the 13 mortar types, 3 cubes of 50 mm side, 3 cylinders of 75 mm diameter and 150 mm length, and 3 prismatic plates of 25 mm × 55 mm × 150 mm were prepared. For each of the two concrete mixes (reference and with RPVC fibres), 8 cubes of 100 mm sides, 3 cylinders of 100 mm diameter and 200 mm length, and 2 prisms of 100 mm × 100 mm × 500 mm, were prepared. All samples were cured under plastic sheets for 24h and removed from the forms thereafter. These were then placed in a moist room at 20°C and 99%RH until they reached 28 days. This curing procedure was employed primarily to ensure hardening of the cementitious mixes through the formation of hydration products from the hydraulic components. After removal from the moist room, the ends of the cylindrical samples were ground to ensure flatness of the surfaces and good contact conditions during testing at 28 days. The dimensions of all samples were carefully measured for appropriate assessment of stress-strain characteristics.

2.3 Testing arrangements

The testing arrangements employed in this study are depicted in Figure 4. For assessing the full stress-strain curve, the compressive strength ($f_{m,cyl}$) and the elastic modulus (E_m) of mortars, Ø75 mm diameter cylinders were tested in a stiff four-post Instron Satec 3500 kN machine. As illustrated in Figure 4a, the samples were placed on the bottom platform of the testing machine. Loading plates of high strength steel were added at both ends of the sample, and a 3D hinge was provided at the top to ensure concentric loading. The sample pre-peak axial behaviour was recorded using three displacement transducers attached to two steel rings positioned symmetrically from the central cross-section at a gauge length of 80 mm. A similar configuration was used to assess the compressive strength of concrete cylinders ($f_{c,cyl}$) of Ø100 mm and their elastic modulus (E_c), noting that the steel rings used to record axial deformations were positioned at 100 mm. Each steel ring was connected directly to the sample through three steel bolts to avoid interaction with the specimen. Three other independent transducers were placed between the machine plates to record the axial deformations. Test measurements were averaged and transformed into strains (ε) by using the measured gauge length for each sample. The load corresponding to the applied displacement was recorded by the machine load cells and transformed into stress (σ) and strength ($f_{i,cyl}$) using the area of the sample.

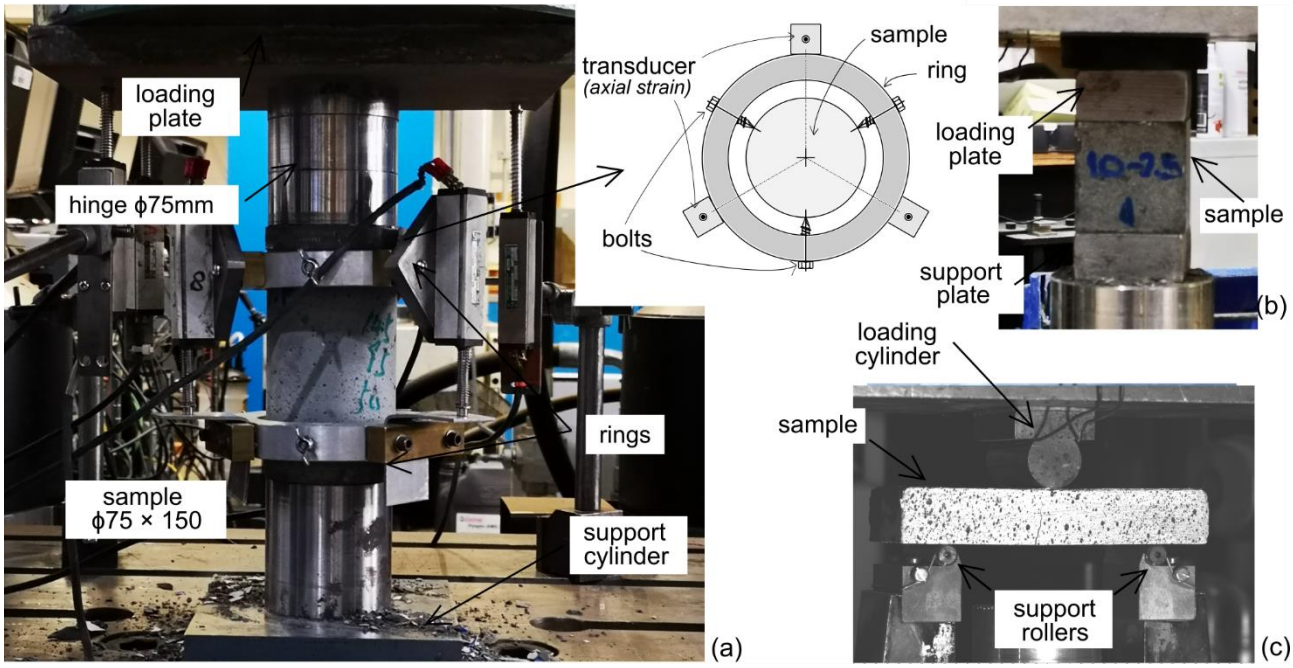


Figure 4 Testing arrangements: a) cylinders, b) cubes, c) prismatic plates

The compressive strength tests on 50 mm mortar cubes ($f_{m,cube}$) and the flexural strength tests on 25×55×150 mm prismatic mortar plates were carried out in displacement control using a two-post displacement control Instron 600 kN machine. To avoid eccentric loading, the testing arrangement included top and bottom high strength steel transfer plates and a hinge (Figure 4b). On the other hand, a purpose-built Instron testing rig was used for three-point bending tests (Figure 4c). The support span for these tests was 100 mm. These values, along with cross-sectional sizes, were used to determine the flexural strength ($f_{m,fl}$) of the materials. Besides the load recorded by the machine, which was used to determine the flexural stress, a digital image correlation (DIC) system was employed for assessing the surface strain characteristics of the prismatic samples [36]. As part of the preparation process, the specimens were firstly painted in white, and then carefully speckled with 0.5-2.0 mm black dots to create a high-contrast black-white pattern (Figure 4c). After testing, the DIC data were processed to obtain deformation vector fields. From these, the crack mouth opening displacement was determined from assigned 20 mm virtual gauges perpendicular to the crack length. Similar testing configurations were used to determine the concrete compressive strength ($f_{c,cube}$) on 100 mm cubes, and the flexural strength ($f_{c,fl}$) from tests on 100 mm square cross-section prismatic samples. A displacement rate of 0.50 mm/min was applied to the specimens tested in compression, whilst a rate of 0.25 mm/min was used for specimens tested in flexure.

3. Characterisation of cementitious RPVC composites

Material characterisation tests on mortar and concrete samples with Reinforced PVC (RPVC) granules resulting from the recycling of end-of-life banners were carried out. Besides the physical

properties, such as hardened density and water absorption presented in Figure 5, the compressive stress-strain and flexural stress-crack opening curves are presented in Figures 6 and 7, respectively. Additional fracture surface properties of the prismatic samples are illustrated in Figure 8, whilst compressive strength and elastic modulus reduction ratios, as well as crushing and fracture energy characteristics, are depicted in Figure 9.

3.1 Density and water absorption

To assess the influence of RPVC proportions on the physical properties of composite RPVC cementitious materials, hardened density and water absorption were determined. The air-dry density of the materials was obtained by dividing the sample mass by its volume, after careful measurement of each sample dimension with a digital calliper. Figure 5a depicts the relative density reduction ratio (ρ/ρ_{ref}) against the volumetric particle replacement ratio ρ_{vp}. The parameter ρ is the density of the sample with RPVC granules, whilst ρ_{ref} is the density of the reference material, without RPVC particles. Considering that ρ_{ref} of mortar was in the range of 2.11 g/cm^3 and of the concrete around 2.35 g/cm^3, a proportional reduction in ρ is observed with $\rho_{vp.}$ There is minimal or no influence in density when ρ_{vp} < 2.5% as ρ/ρ_{ref} = 1.00 both for mortars and concrete. The reduction in ρ is on average about 1% for ρ_{vp} = 5%, 3% for ρ_{vp} = 10%, and 8% for ρ_{vp} = 20%, respectively.

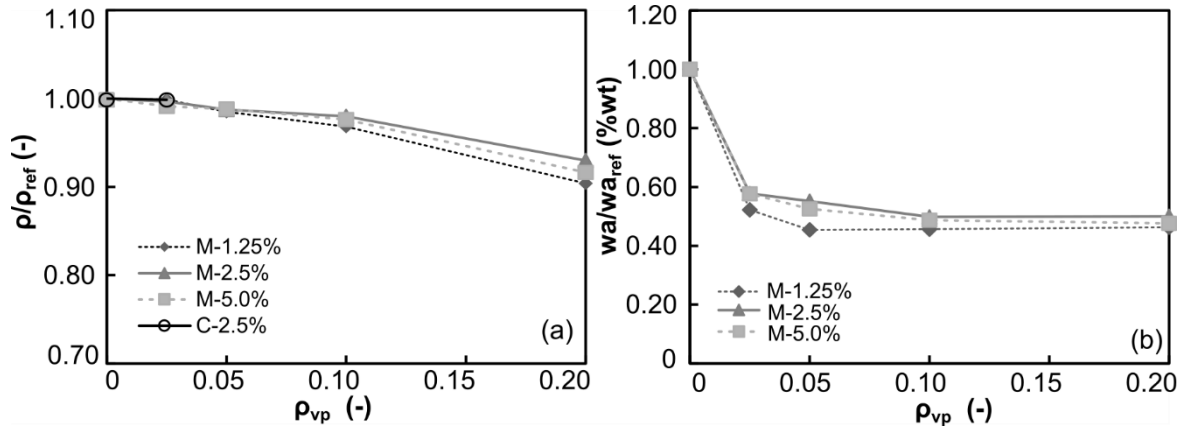


Figure 5 Relationship between replacement ratio and: a) density; b) water absorption

It can also be observed from Figure 5a that the particle size has some slight influence on the density, with samples incorporating the smallest particle size (1.25 mm < dp < 2.50 mm) showing the lowest density. This may be associated with a higher porosity of the hardened material which results from the formation of a higher number of pores near the RPVC granules in comparison to the other mixes with intermediate and relatively large RPVC particles.

In addition to density, the water absorption properties were assessed by drying the mortar samples to constant weight using an oven at 95°C and then by immersing them in water for 24 hours. Figure 5b depicts the water absorption properties in percentage by weight (wt%) in comparison with the

volumetric particle replacement ratio ρ_{vp}. As shown in the figure, the (wa/wa_{ref}) ratio in which 'wa' is the value for RPVC composite whilst the subscript 'ref' indicates the reference mortar, decreases to about 0.5 for all RPVC materials. The water absorption of the reference mortar is consistently above 4.5%, whilst that of RPVC mortars varies between 2.11-2.68%.

3.2 Compressive stress-strain response

The average stress-strain (σ-ε) curves of RPVC mortars with three distinct particle sizes (d_p) and varying replacement ratios (ρ_{vp}), as determined from uniaxial tests on cylindrical specimens, are presented in Figures 6a,b,c. Figure 6d illustrates the relative strength reduction ($f_{i,cyl}/f_{i,cyl,ref,}$) where i=m,c) as a function of ρ_{vp} both for the mortar (m) and concrete (c) materials investigated herein. The strength characteristics are also given in Table 2. As observed in Figure 6, the reference mortar CM-0-0 had an average compressive strength of $f_{m,cyl}$=64.7 MPa and a brittle response as the post-peak σ-ε shows a sudden drop in σ after the peak strength is reached. As ρ_{vp} increases, there is a reduction in $f_{m,cyl,}$ yet with an enhancement in ductility, as reflected in the softer post-peak σ-ε.

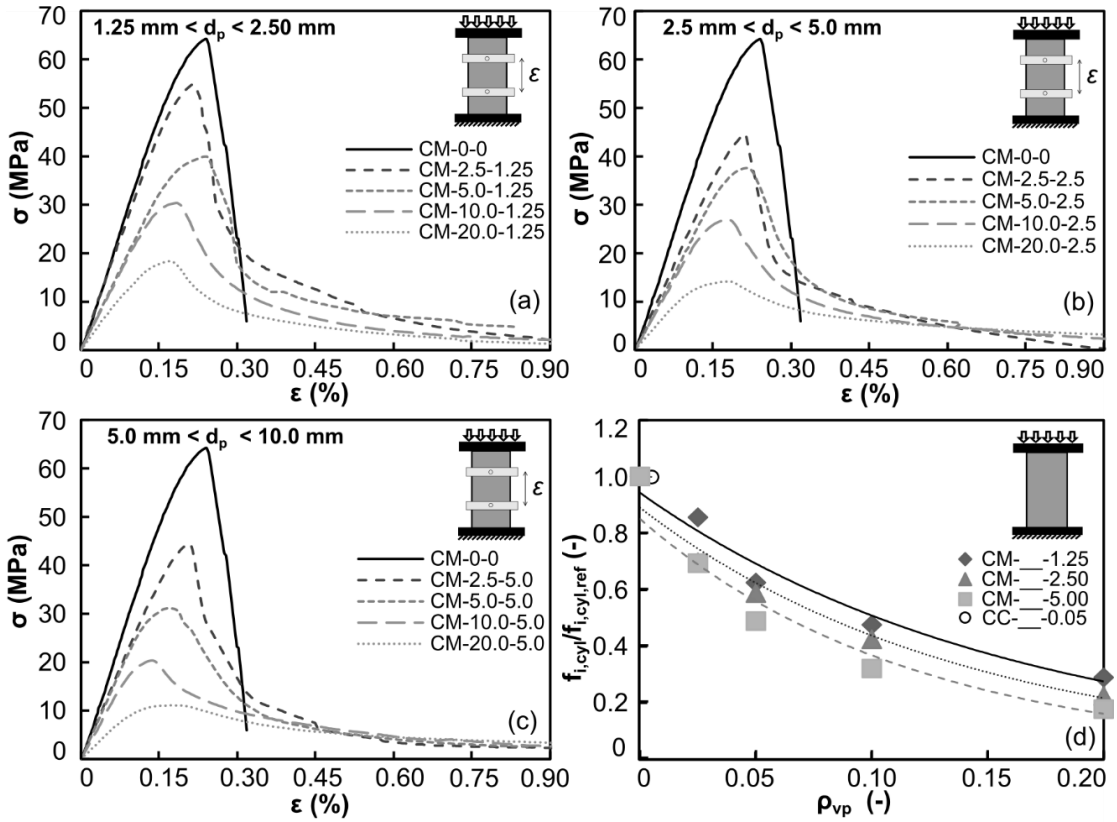


Figure 6 Stress-strain response of RPVC mortars with granule sizes of: a) 1.25 mm > d_p > 2.50 mm, b) 2.50mm > d_p > 5.0 mm, c) 5.0 mm > dp > 10.0 mm; d) compressive strength reduction ratios

After reaching the crushing strain (ε_{c1}), the concrete cylinders split into two distinct bodies separated by a macro-crack which was subjected to sliding. The sliding response depends on the characteristics of the crack interfaces. In the case of mortar and concrete samples, sliding is restricted by the roughness of the cementitious matrix and physical protrusions from the aggregates. As for mortars in which only fine aggregates are present, the physical protrusions are limited and, after crushing, the two bodies slide instantaneously. In contrast, RPVC granules and fibres act as bridging elements, counteracting the dislocation of the two bodies and reducing the brittleness of the material as indicated by the assessments of crushing energy described below.

In terms of mechanical properties, the test results indicate that for each increment of 10% replacement the corresponding $f_{m,cyl}$ is halved, as a function of the type of replacement RPVC granules. For example, for ρ_{vp} =2.5% (i.e CM-2.5), the reduction in strength is between 15-30% of its reference mortars. An increase of ρ_{vp} to 5.0% (CM-5.0) leads to a $f_{m,cyl}/f_{m,cyl,ref}$ ratio in the range of 0.49-0.62 (the loss of strength is between 38-51%). The compressive strength $f_{m,cyl}$ of cylinders with ρ_{vp}=10% (CM-10) is between 0.32-0.47 of CM-0-0. Ultimately, for 20% replacement (CM-20), $f_{m,cyl}$ is less than a quarter of $f_{m,cyl,ref.}$. On the other hand, $f_{m,cyl}$ reduction in concrete with 0.5% fibres (CC-0.2-0.05) is below 1% in comparison to its reference counterpart (CC-0-0).

Table 2 Mechanical properties of RPVC mortars

	$f_{m,cyl}$ (MPa)		$f_{m,fl}$ (MPa)		E_m (GPa)	
Group	(a)/(b)/(c)	Average	(a)/(b)/(c)	Average	(a)/(b)/(c)	Average
M-0-0	66.6/62.6/64.9	64.7±2.0	6.64/6.78/6.12	6.51±0.3	31.9/33.1/32.2	32.4±0.6
M-2.5-1.25	54.8/56.8/54.9	55.5±1.1	6.59/6.92/6.53	6.68±0.2	30.4/30.0/32.1	30.9±1.0
M-2.5-2.5	40.3/43.9/49.6	44.6±4.6	5.47/5.58/5.98	5.67±0.2	21.4/23.9/25.0	23.5±1.8
M-2.5-5.0	48.9/48.3/46.1	47.7±1.4	7.16/5.08/5.73	5.99±1.0	26.4/21.4/26.4	24.7±2.8
M-5.0-1.25	45.2/37.3/40.4	41.0±3.9	5.99/5.07/5.53	5.53±0.4	24.8/19.5/22.8	22.4±2.6
M-5.0-2.5	38.5/35.8/38.6	37.6±1.6	6.22/5.77/6.58	6.19±0.4	24.1/17.2/22.1	21.1±3.5
M-5.0-5.0	29.6/29.8/35.8	31.7±3.5	6.38/5.92/5.47	5.92±0.4	23.9/21.7/26.3	24.0±2.2
M-10-1.25	30.4/29.9/30.7	30.4±0.4	4.70/4.65/4.48	4.61±0.1	21.4/21.4/21.0	21.3±0.2
M-10-2.5	28.1/23.6/30.3	27.3±3.4	3.94/4.42/4.52	4.29±0.3	19.8/17.9/20.4	19.4±1.2
M-10-5.0	18.4/23.8/18.9	20.4±2.9	4.37/4.73/4.55	4.55±0.1	19.3/18.3/22.8	20.1±2.3
M-20-1.25	18.0/21.2/15.9	18.4±2.6	3.49/3.83/3.16	3.49±0.3	12.5/21.6/12.9	15.7±5.1
M-20-2.5	14.4/13.7/14.4	14.2±0.4	2.61/3.92/3.70	3.41±0.7	12.0/12.9/12.5	12.5±0.4
M-20-5.0	10.2/13.0/10.4	11.2±1.5	4.48/4.01/3.74	4.08±0.3	7.0/10.2/17.4	11.5±5.3
C-0-0	71.0/69.1/72.9	71.0±2.7	5.81/7.08/-	6.40±0.9	47.7/48.2/48.7	48.2±0.5
C-0.5-0.05	71.1/70.8/69.5	70.5±0.8	6.10/6.64/-	6.40±0.4	48.2/48.1/47.8	48.0±0.2

The strength reduction occurs primarily as the RPVC particles are softer than sand, and also due to the hardened matrix interaction properties of the RPVC particles at the interface transmission zone. As shown in Figure 6d, the $f_{m,cyl}$ depends both on the replacement ratio and the RPVC particle size (d_p). Large plastic particles with sizes of 5.0 mm < d_p < 10.0 mm had the strongest effect in terms of strength reduction, whilst those with relatively small diameters (1.25 mm < d_p < 2.50 mm) had the lowest impact. Smaller particles blend in a better manner with the remaining mix constituents creating a more homogenous mix in comparison to large particles. The latter are more dispersed and have a higher surface area which produces a less homogenous mix. Close inspection of the particle distribution throughout the failure surfaces of the tested cylinders and cubes showed a relatively uniform distribution. The cylinders had generally shear and cone failures with diagonal cracks passing through the centre of the samples, whilst the cubes had hourglass type failures. Such characteristics were observed for all tests regardless of the replacement ratio and granule size, and agree with failure modes for conventional concrete and mortar.

3.3 Flexural behaviour

To determine the flexural strength and fracture characteristics of RPVC mortars, three prismatic plates for each mortar mix have been tested under three-point bending. For brevity, only average test flexural stress (σ_{fl}) – crack mouth opening (w) are presented in Figure 7, whilst flexural strengths are given in Table 2. Figures 7a,b,c depict the σ_{fl} - w for mortars with three distinct RPVC particle sizes (d_p) and varying replacement ratios (ρ_{vp}), whilst Figure 7d shows the relative strength reduction ratios ($f_{fl,i}/f_{fl,i,ref}$ where i=m,c) as a function of ρ_{vp} both for mortar (m) and concrete (c). Additional images with the fracture surfaces of the flexural specimens are shown in Figure 8.

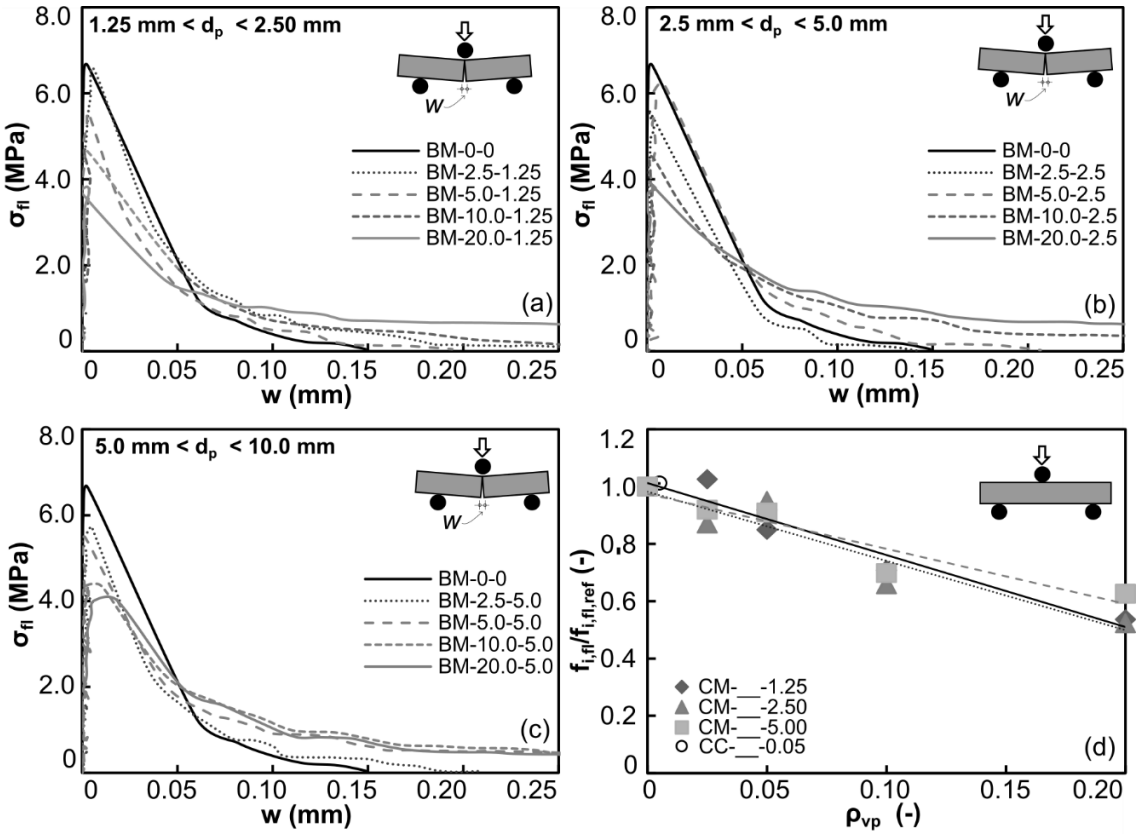


Figure 7 Flexural stress (σ_{fl}) – crack width (w) relationship for mortars with granule sizes of: a) 1.25 mm > d_p > 2.50 mm, b) 2.50mm > d_p > 5.0 mm, c) 5.0 mm > dp > 10.0 mm; d) flexural strength reduction ratios

As mortar and concrete materials have very poor capacity in tension and practically no ductility, the high strength samples without RPVC (i.e. BM-0-0) failed nearly instantaneously after the peak flexural strength was reached ($f_{m,fl}$), with a sudden drop in σ_{fl} to about $0.15 \times f_{m,fl}$. Samples with RPVC granules had some residual strength and enhanced softening, proportional to the increase in replacement ratio (ρ_{vp}). The highest improvement in post-peak response was obtained for samples with the largest ρ_{vp} (i.e. BM-20.0) as indicated by the continuous grey curves in Figures 7a,b,c. This is attributed to the clamping action produced by the RPVC particles which limited the crack width opening in the softening regime. As indicated in the figure, the size of the plastic particle (d_p) had a minimal effect on the post-peak response and some influence in terms of $f_{m,fl}$.

Figure 8 illustrates the fracture surfaces of selected flexural mortar samples. As indicated, an increase in ρ_{vp} (from top to bottom of the figure) results in a higher agglomeration of RPVC granules within the cross-section. Although the granule distribution within the cross-section has some influence on the post-peak response, the matrix-RPVC granule bonding surface would be very similar for each ρ_{vp} and different d_p. After cracking, as the forces are transferred through the compression zone and in tension through the bond between the granules and the matrix, the post-peak response is the same. This is noted below and in Figure 9, in terms of the post-peak fracture energy, which is largely the same for the same ρ_{vp}, irrespective of the particle size (d_p). The RPVC

granule - matrix bond strength is dependent on the embedment length of the granule. For fibres, as shown in Figure 2d, which due to their aspect ratio have a relatively longer embedment length than the granules in Figure 2a,b,c, the post-peak enhancement is significantly higher.

The flexural strength reduction ratios of RPVC mortars ($f_{m,fl}/f_{m,fl,ref}$) with respect to ρ_{vp} show lower values compared to the case of compressive strength reduction trends. For the highest level of ρ_{vp}=0.2 (BM-20), the $f_{m,fl}/f_{m,fl,ref}$ ratio is between 0.52-0.63. This corresponds to more than half the average strength of the reference samples (i.e. ρ_{vp}=0 - BM-0), whilst the compressive strength reduction is up to 80% of its reference material. As indicated in Figure 7d, the $f_{m,fl}/f_{m,fl,ref}$ ratio is 0.66-0.71 for ρ_{vp}=0.1 (BM-10), increases to 0.85-0.95 for ρ_{vp}=0.05 (BM-5.0), and is 0.94 on average for ρ_{vp}=0.025 (BM-2.5). On the other hand, the presence of a very small quantity of fibres of 0.5% in RPVC fibre-concrete (CC-0.5-0.05) leads to a reduction below 1% of $f_{c,fl}$ in comparison to its conventional counterpart (C-0-0). As shown in the figure, for the same ρ_{vp}, the reduction factors for $f_{c,fl}$ are higher than those for compressive strength, indicating a more effective use of RPVC cementitious composites in structural members subjected primarily to bending.

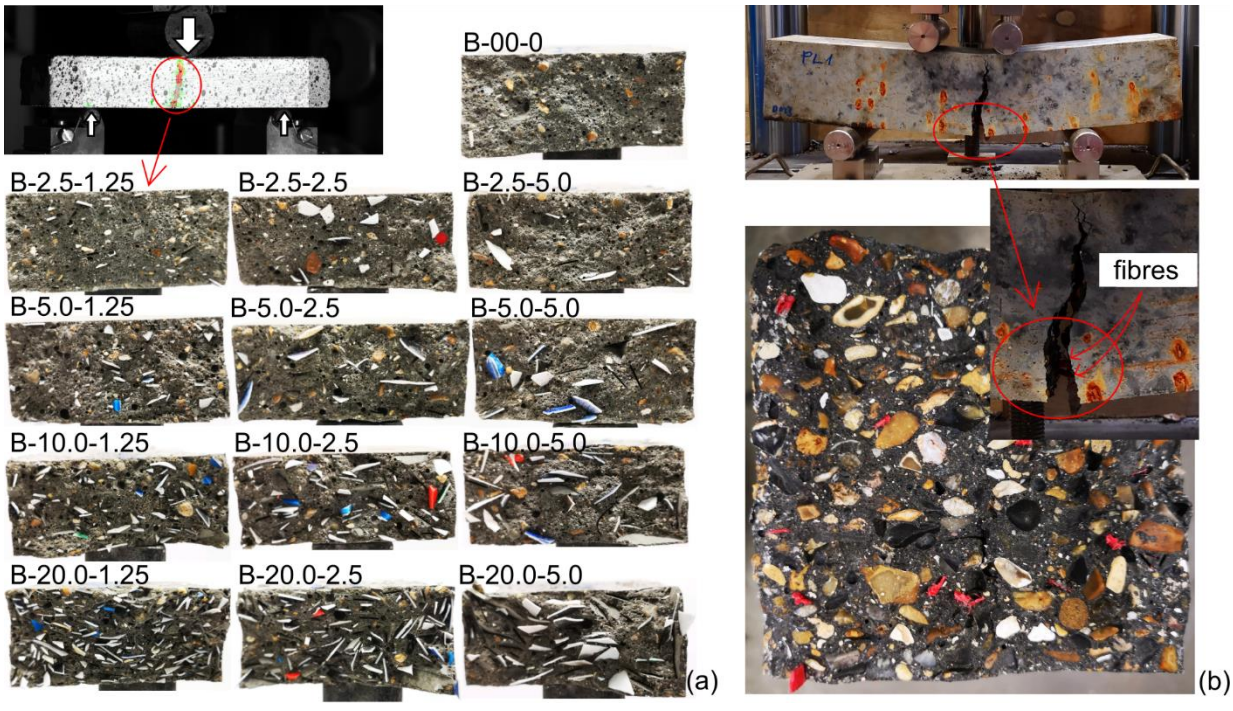


Figure 8 Fracture surface properties for: a) mortars, b) concrete

3.4 Comparative assessments

In addition to the cylindrical specimens used to assess the σ-ε response of RPVC composites, as depicted in Figure 6 and described in Section 3.2, three cubic samples were tested in compression

for each mix. This enabled a direct correlation between the cylindrical and cubic compressive strengths. As depicted in Figure 9a, the compressive strength reduction factors ($f_{m,cube}/f_{m,cube,ref}$) resulting from cube tests are higher than those from cylinders ($f_{m,cyl}/f_{m,cyl,ref}$). As for the cases described in the previous section, the compressive strength reduction is largely proportional to the replacement ratio $\rho_{vp,}$ with some slight influence from the RPVC particle size (d_p). It is shown that smaller RPVC particles (1.25 mm < d_p < 2.50 mm - Specimens SM-2.5-1.25, SM-5.0-1.25, SM-10-1.25, SM-20-1.25) had the lowest effect, showing on average the higher $f_{m,cube}/f_{m,cube,ref}$ ratios, whilst relatively large granules (5.0 mm < d_p < 10.0 mm - Specimens SM-2.5-5.0, SM-5.0-5.0, SM-10-5.0, SM-20-5.0) had the lowest $f_{m,cube}/f_{m,cube,ref}$ ratios (Figure 9a). The conversion ratios between cubic to cylindrical strength $f_{m,cube}/f_{m,cyl}$ vary proportionally from 1.0 to about 1.5 with the replacement ratio $\rho_{vp,}$ indicating a higher effect of confinement for larger proportions of RPVC granules.

The compressive tests on cylinders also permit an assessment of the elastic modulus of RPVC materials. This was determined in the 0.3-0.5×$f_{i,cyl}$ stress range, where $f_{i,cyl}$ is the specimen strength, as the σ-ε curves exhibit relatively linear response. The complete elastic modulus values are presented in Table 2, whilst modulus reduction factors ($E_i/E_{i,ref}$) are depicted in Figure 9b. As for the cylindrical compressive strength, the particle size had some influence on the ($E_i/E_{i,ref}$) ratios. For ρ_{vp} =0.2, smaller RPVC particles (1.25 mm < d_p < 2.50 mm - Specimens CM-2.5-1.25, CM-5.0-1.25, CM-10-1.25, CM-20-1.25) had ($E_i/E_{i,ref}$) ratios above 35% of those with relatively large granules (5.0 mm < d_p < 10.0 mm, Specimens CM-2.5-5.0, CM-5.0-5.0, CM-10-5.0, CM-20-5.0). Similar trends are also observed for intermediate ρ_{vp} ratios. These observations, along with those from the assessment of the σ-ε curves and compressive tests on cubes, indicate that smaller particle sizes have less influence on the degradation of elastic and compressive strength properties of RPVC cementitious composites.

The above observations are counterbalanced to some extent by the performance in the post-peak regime, where the crushing energy G_c assessments in Figure 9c indicate contrasting behaviour. The crushing energy was determined herein as the area under the post-crushing σ-ε. As noted before in Section 3.2, there is a steady reduction in $f_{m,cyl}$, and an enhancement in ductility represented by a softer post-peak σ-ε, with the increase in the replacement ratio (ρ_{vp}). The intermediate and large particles sizes (Specimens CM-2.5-2.5, CM-5.0-2.5, CM-10-2.5, CM-20-2.5, CM-2.5-5.0, CM-5.0-5.0, CM-10-5.0, and CM-20-5.0) seem to perform better, as the $G_c/G_{c,ref}$ ratios are higher by a factor above 3.5 in comparison to the those with smaller particles (Specimens CM-2.5-1.25, CM-5.0-1.25, CM-10-1.25, CM-20-1.25) which show decreasing $G_c/G_{c,ref}$ ratios for higher ρ_{vp} and with values below 2.6. On the other hand, the fracture energy (G_f) properties depicted in Figure 9d seem to be influenced to a lesser extent by the particle size. A relatively steady improvement in $G_c/G_{c,ref}$ ratios

occurs with an increase in ρ_{vp}. This indicates an improved post-cracking performance when RPVC granules are present.

As shown before, smaller particles had a relatively long acicular or triangular geometry, in comparison to intermediate and large size granules, hence act as fibres which inherently have a higher relative embedment length and improved bond properties. These performance characteristics have been confirmed using a very small proportion of RPVC macro-fibres which acted as bridging mechanisms for the opened cracks and provided the RPVC concrete composite with significant residual strength. Such behaviour has also been observed in concrete elements reinforced with relatively low strength PET or HDPE fibres [19, 37, 38] and relatively high strength PP fibres used in railway sleepers and concrete pipes [39, 40]. Low-strength fibres typically affect the mechanical properties, but they provide mortar and concrete with reduced water permeability as well as enhanced plastic shrinkage, flexural toughness and post-cracking performance [19, 26].

Based on the experimental findings, it can be concluded that RPVC granules with fibre-like aspect ratios, can be effectively used in flexurally-dominated elements such as pavements, footpaths and sleepers, among others, in proportions up to 10%. Such fibres typically contribute to material ductility and may also be suitable in structural elements. In relative terms, a higher efficiency would be obtained for lower reference mortar or concrete strengths as the relative reduction in mechanical properties would be less. However, there are several challenges that need to be addressed to enable reliable application of RPVC granules in practice, including: (i) characterisation of recycled banners in terms of strength, stiffness, and durability; (ii) automated processing of recycled banners in granules or fibres in a standardised manner; (iii) assessment of fibre-concrete bond properties, mix workability and homogeneity.

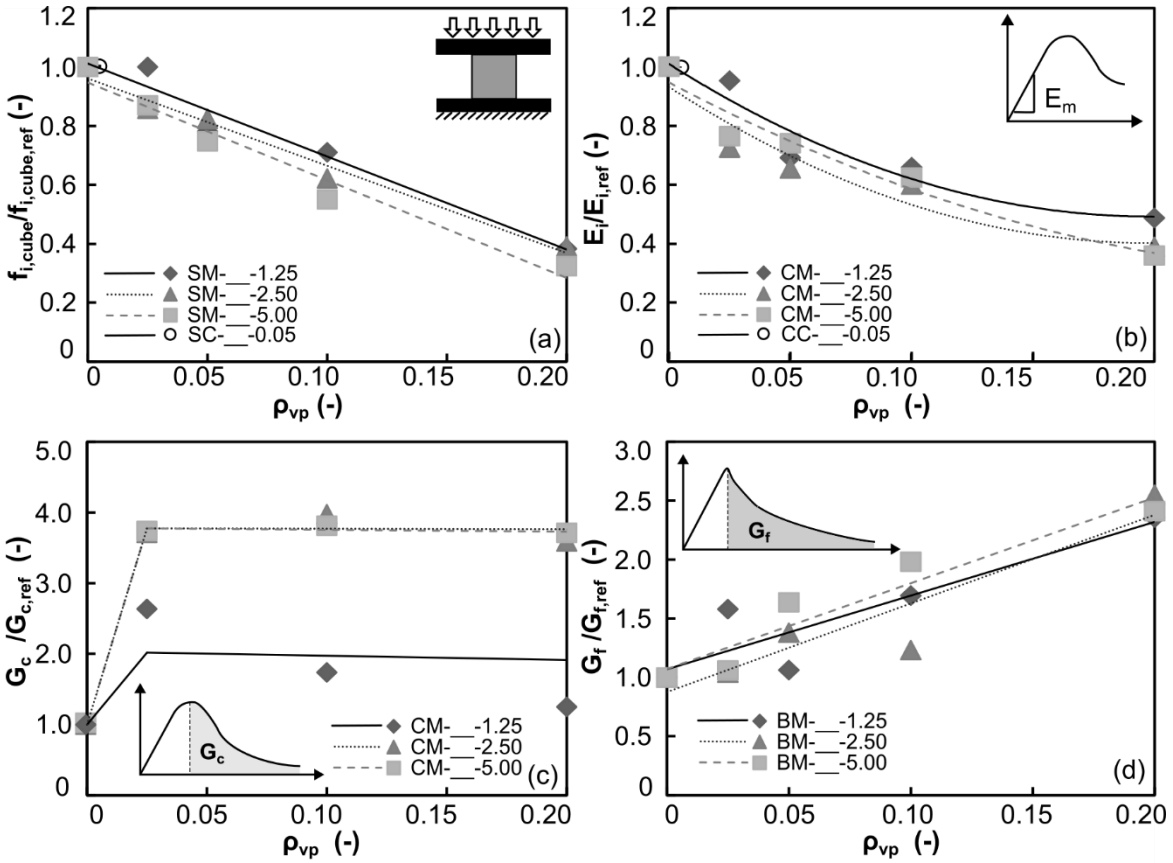


Figure 9 Relationship between replacement ratio and: a) cubic compressive strength, b) elastic modulus, c) crushing energy, d) fracture energy

4. Analytical representations

4.1 Mechanical properties

In addition to the experimental results described above, a database of cementitious composite incorporating waste plastics in various proportions has been collated. This consists of a total of more than 80 mixes corresponding to a minimum of 240 compressive tests, in which mineral aggregates are replaced in proportions of up to 50% with granules, particles or aggregates resulting from the recycling of Polyethylene Terephthalate (PET) [17, 41-45], Polycarbonate (PC) [45,46], Polystyrene (PS) [28], High Impact Polystyrene (HIPS) [47], or cross-linked Polyethylene (XLPE) [48], together with the reinforced Polyvinyl chloride (RPVC) from this paper. The cylinder compressive strength of the reference material was between f_{c0}=22.8-64.7 MPa, whilst the average was in the range of 39.3 MPa. It is worth noting, that when cylindrical strength was not available, a conversion factor of 0.8 was applied to the cubic strength [49]. In most cases, fine mineral aggregates were replaced with plastic particles up to 5 mm. The database enables the validation of expressions presented below against wider ranges of constituent parameters than those reported in Sections 2 and 3 of this paper.

To represent the compressive strength degradation ratio (f_{pc}/f_{c0}) of cementitious composites incorporating waste plastics, Equation (1) is proposed. This is a function of the reference material strength (f_{c0}) from which the cementitious composite with plastics has been derived, the compressive strength of the composite with plastics (f_{pc}), the volumetric replacement ratio (ρ_{vp}) and a parameter 'λ' that depends on the physical, mechanical, and surface properties of the replacement plastic aggregates. The typical ranges of λ, depicted by Equation (2), vary between 0.90 and 2.50. The higher bound (λ=2.50) indicates a more significant strength reduction with an increase in ρ_{vp}, whilst λ=0.90 is associated with a lower influence of plastic aggregates on the compressive strength of the composite. Mixes from the database with PC, PS, HIPS, XLPE, and in some cases with PET, are well represented by λ=0.90, whilst, mixes with PET, LDPE, RPVA by λ=2.50, respectively.

As shown in Figure 10a, there is a larger variation in how PET aggregates influence the strength properties compared with other plastics, and this is primarily related to the surface properties of the aggregates and their size distribution. Such variations can also be attributed to testing arrangements, loading procedures and specimen sizes [50,51]. As shown in the same figure, for the mixes with small RPVC granule size d_p (1.25 mm > d_p > 2.50 mm), investigated in this paper, λ=0.90 ensures reliable predictions of the compressive strength degradation factor. In practice, this parameter can be obtained by assessing the compressive strength properties of the reference material and a case with plastic aggregates through testing. A direct comparison between the database f_{pc}/f_{c0} values and those predicted by Equation (1) indicates that the COV is about 18% and the test-to-predicted ratio is 1.07, which are within expected ranges with good control of testing parameters [50].

$$f_{pc} = \frac{1}{1+5\lambda\rho_{vp}} f_{c0} \tag{1}$$

$$\lambda = \begin{cases} \min = 0.90 \rightarrow PC, PS, HIPS, XLPE \\ avg = 1.35 \rightarrow database \\ \max = 2.50 \rightarrow RPVC, LDPE, PET \end{cases} \tag{2}$$

Using available data from the tests carried out in this study as well as those from the database, Equation (3) is proposed to predict the elastic modulus E_{pc} of the plastic-cementitious composite based on the f_{pc} value obtained with Equation (1). Similarly, Equations (4) and (5) are proposed to predict the splitting tensile $f_{pct,sp}$ and flexural strength $f_{pct,fl}$, respectively, for a cementitious composite with plastic aggregates. It is worth noting that the splitting strength is directly equivalent to uniaxial tensile strength [52]. A comparison between the predictions of Equations (3)-(5) and the

database test results is presented in Figures 10b-d, indicating good agreement between the tests and predictions, with a COV of 12-14% and a test-to-predicted average of 1.00-1.06.

$$E_{pc} = 11\left(\frac{f_{pc}}{10}\right)^{2/3} \tag{3}$$

$$f_{pct,sp} = 0.32\, f_{pc}^{\,2/3} \tag{4}$$

$$f_{pct,fl} = 0.45\, f_{pc}^{\,2/3} \tag{5}$$

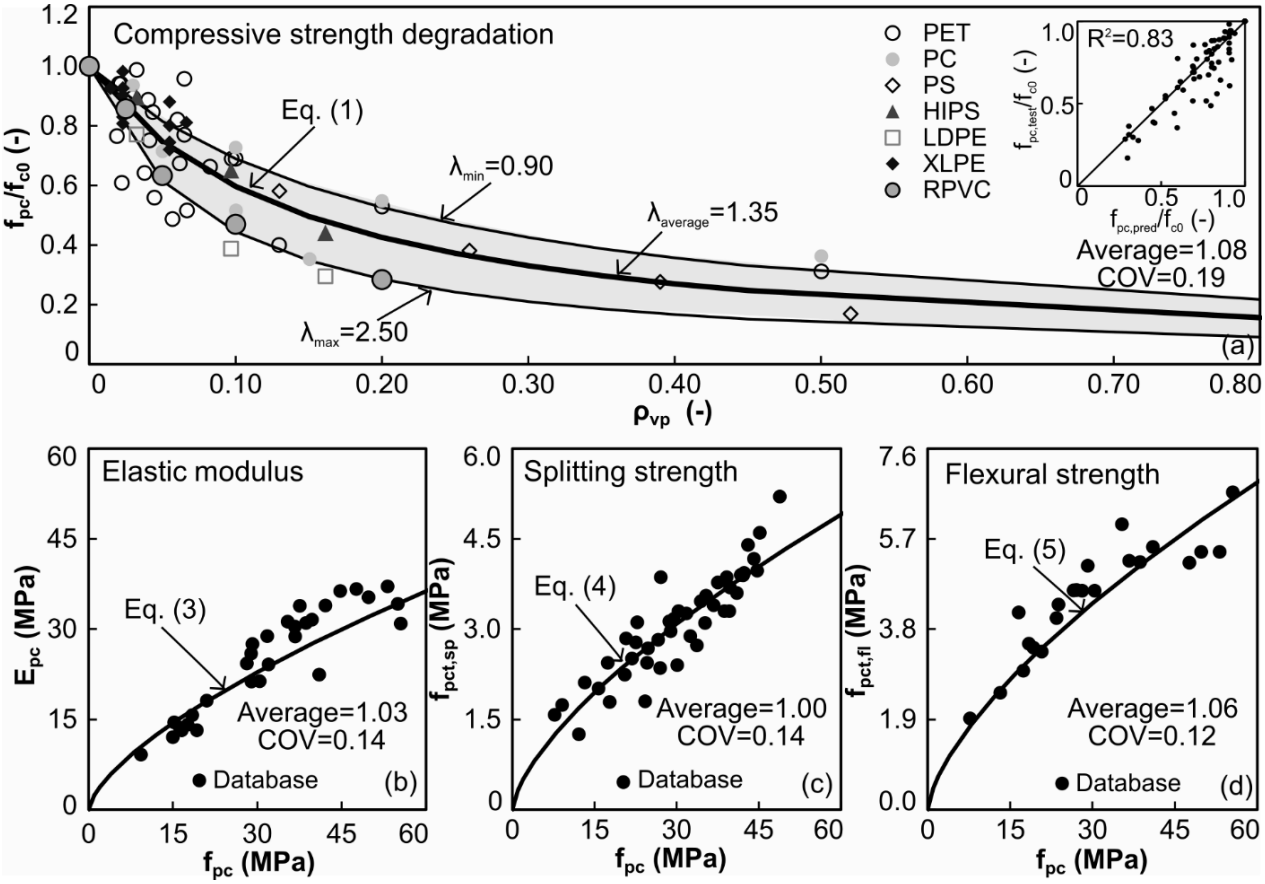


Figure 10 a) Compressive strength degradation as a function of volumetric replacement ratio; Relationship between compressive strength and: b) elastic modulus, c) splitting strength, d) flexural strength

As described above, the test results from this paper together with those from the collated database enabled the definition of a series of analytical expressions for assessing the main mechanical properties (f_{pc}, E_{pc}, $f_{pct,sp}$ and $f_{pct,fl}$) of cementitious composites provided with plastic aggregates. The proposed equations capture the influence of the type and content (i.e. ρ_{vp}) of plastics, and can be used to assess the full constitutive properties of plastic-cement composites, as discussed below.

4.2 Constitutive modelling

This section introduces a full constitutive model that can be employed for modelling the compressive stress-strain and tension stress-crack width opening response of cementitious composites incorporating plastic aggregates. The compressive behaviour can be predicted from Equations (6-8) using a three-range closed-form representation, as illustrated in Figure 11a. The proposed model is a modified version of an existing model developed by the authors for cementitious composites incorporating rubber particles [12]. The first range up to $\varepsilon_{pc,el}$ is associated with proportionality between stresses and strains (Equation 6), limited by a stress-to-strength ratio $\sigma_c/f_{pc}=0.3$. In this equation, f_{pc} is the compressive strength estimated using Equation (1) and E_{pc} is the elastic modulus estimated from Equation (4). The second range, between the proportionality limit $\varepsilon_{pc,el}$ and the crushing strain ε_{pc1}, follows a second degree polynomial representation (Equation 7a). The crushing strain ε_{pc1} can be determined from Equation (7b) which is a function of the replacement ratio ρ_{vp} and the crushing strain of the reference material [49]. The post-peak range, which can be predicted from Equation (8a,b), is limited by the ultimate strain $\varepsilon_{pu.}$ This expression was obtained by assuming a triangular distribution of the crushing energy, depicted in Figure 11a.

$$\frac{\sigma_c}{f_{pc}} = E_{pc}\varepsilon f_{pc} \rightarrow \varepsilon \le \varepsilon_{pc,el} = 0.3 f_{pc} / E_{pc} \tag{6}$$

$$\frac{\sigma_c}{f_{pc}} = \frac{5}{3}\left(\frac{\varepsilon-\varepsilon_{pc,el}}{\varepsilon_{pc1}}\right) - \left(\frac{\varepsilon-\varepsilon_{pc,el}}{\varepsilon_{pc1}}\right)^2 + 0.3 \rightarrow \varepsilon_{pc,el} < \varepsilon_{pc1} \le \varepsilon_{pc1} \tag{7a}$$

$$\text{where } \varepsilon_{pc1} = 0.95\left(1-\rho_{vp}\right)\varepsilon_{c0,1} \text{ and } \varepsilon_{c0,1} = 0.7 f_{c0}^{\ 0.31} \tag{7b}$$

$$\frac{\sigma}{f_{pc}} = \frac{1}{8}\left(\frac{f_{pc}^{\ 1/3}}{(1+\rho_{vp})^{2/3}}-1\right)\left(\frac{\varepsilon}{\varepsilon_{pc1}}-1\right)^2 - \frac{6}{8}\left(\frac{f_{pc}^{\ 1/3}}{(1+\rho_{vp})^{2/3}}-1\right)\left(\frac{\varepsilon}{\varepsilon_{pc1}}-1\right) + \frac{f_{pc,2}}{f_{pc}} \rightarrow \varepsilon_{pc1} < \varepsilon \le \varepsilon_{pcu} \tag{8a}$$

$$\text{where } \frac{f_{pc,2}}{f_{pc}} = \frac{5}{3}\left(1-\varepsilon_{pc,el}/\varepsilon_{pc1}\right) - \left(1-\varepsilon_{pc,el}/\varepsilon_{pc1}\right)^2 + 0.3 \tag{8b}$$

The tension-governed behaviour of cement-based materials is typically represented by a linear elastic regime up to peak (i.e. f_{pct} for tensile strength, $f_{pct,sp}$ for splitting strength, $f_{pct,fl}$ for flexural strength) and a non-linear softening regime (Figure 11b). The elastic regime up to peak strength is represented by a proportionality relationship (Equation 9). Direct tension tests on plastic-cementitious composites are lacking, and existing information regarding the tension-governed behaviour is typically obtained from splitting and flexural tests. Close inspection of the results obtained from the flexural tests indicated that the ultimate crack mouth displacement of the reference material, without plastic granules, was $w_{max,0}$=0.15 mm. Both this value and the softening properties are in close agreement with direct tension tests from the literature [53].

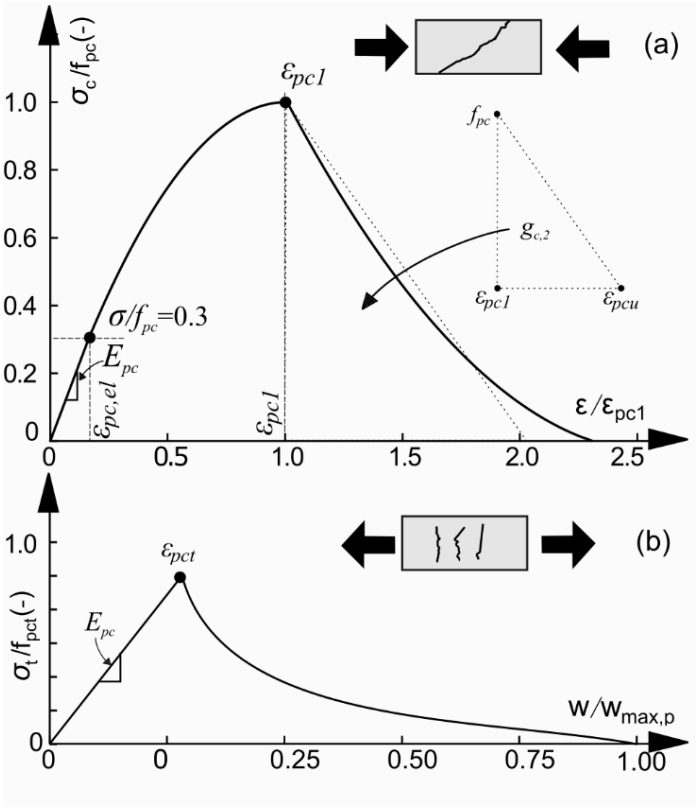


Figure 11 Constitutive modelling in a) compression, b) tension

It is hence considered that the softening behaviour obtained from flexural tests would be representative for modelling the response of plastic-cement-based composites in tension. To this end, Equation (10a) which employs an inverse power function is proposed to model the post-peak tension response of the material. This is a function of the ρ_{vp}-dependent λ_{pw} parameter (Equation 10b) and the ultimate crack displacement $w_{max,p}$ of the composite (Equation 10c). The latter is also a function of ρ_{vp} and was calibrated against the test results from this paper.

$$\frac{\sigma_c}{f_{pct}} = E_{pc}\varepsilon f_{pct} \rightarrow \varepsilon < \varepsilon_{pct} = f_{pct} / E_{pc} \tag{9}$$

$$\frac{\sigma_t}{f_{pct}} = \frac{1}{1+5\left[\lambda_{pw}\left(w/w_{max,p}\right)\right]^{5/4}} \rightarrow \varepsilon \geq \varepsilon_{pct} \tag{10a}$$

$$\lambda_{pw} = 2.5\left(9\rho_{vp}+1\right) \tag{10b}$$

$$w_{\max,p} = w_{\max,0} + 2\rho_{vp}\left(5\rho_{vp}+1\right) \text{ and } w_{\max,0} = 0.15\,\text{mm} \tag{10c}$$

Figure 12 illustrates the predicted constitutive response using Equations (6-10) compared with test curves for RPVC materials with small granule size (1.25 mm > d_p > 2.50 mm), as these offered the best performance and are recommended for practical application. As shown in Figure 12a, the predicted compressive stress-strain response (shown as continuous curves) fits well within the experimental ranges (depicted as grey curves and areas). Notably, the predicted compressive strengths are close to the test averages, whilst the stiffness, crushing strain and post-peak response are largely within the experimental ranges. The predicted inelastic flexural behaviour (shown in Figures 12b-d) is in good agreement with test curves, particularly for stress-to-strength ratios above 10%, with some variation for lower ratios.

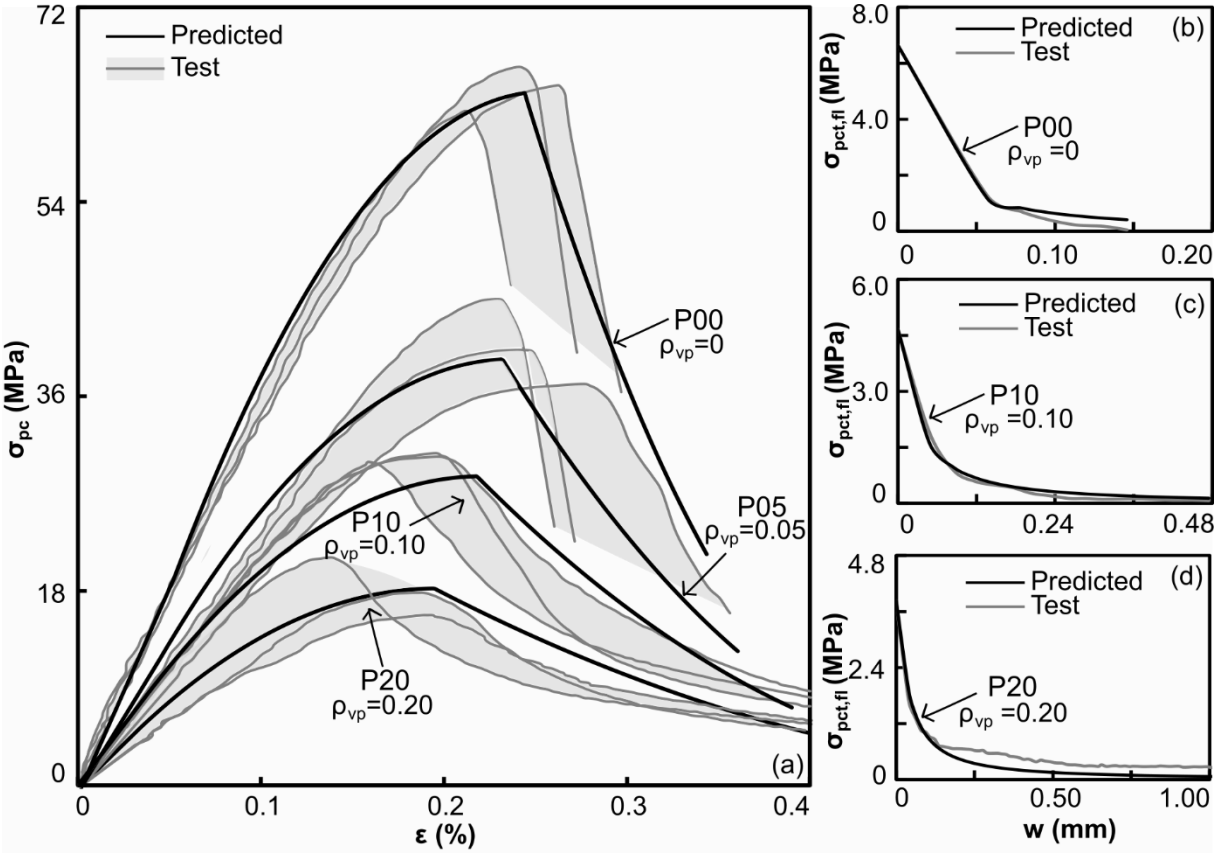


Figure 12 Comparative assessment between test results and predictions for: a) stress-strain curves in compression for ρ_{vp}=0-0.20; stress-crack mouth opening in flexure for: b) ρ_{vp}=0, c) ρ_{vp}=0.10, d) ρ_{vp}=0.20

The predictions in Figure 12, along with the statistical results in Figure 10, indicate that the constitutive expressions (Equations 1-5) and the full constitutive model (Equations 6-10) can be used to determine the response of cementitious composites incorporating plastic particles. The closed-form representations proposed above offer a reliable and practical approach for determining the main mechanical properties for design purposes. On the other hand, the full constitutive response are necessary for nonlinear analysis purposes, and for undertaking parametric investigations into the structural response of members incorporating materials with alternative aggregates from waste materials [54-57]. The constitutive parameters from Equation (2) can be directly applied to obtain the full constitutive response provided that the composite mix and plastic aggregate properties are similar to those considered in this paper and within the collated database.

As noted in Section 3.2, the compressive strength reduction occurs primarily as the RPVC particles are softer than sand, and also due to the hardened matrix interaction properties of the RPVC particles at the interface transmission zone. Plastic particles such as those used in this investigation are of a hydrophobic nature, hence, restricting water movement within the matrix. Ultimately this inhibits hydration and generates a higher amount of free water in the matrix [58, 59]. Microstructural investigations showed that the free water around plastic particles increases proportionally with the replacement ratio, weakening the plastic-paste interface and producing a greater number of voids [60]. The interface properties depend on the type of plastic and particle size [58]. A relatively smoother surface of PVC aggregates compared to the natural sand seems to be the reason behind the plastic granule - matrix bond reduction, ultimately having a negative influence on the compressive strength [61]. This has been observed in this paper and noted in Section 3.2. Large plastic particles with sizes of 5.0 mm < dp < 10.0 mm had the strongest effect in terms of strength reduction, whilst those with relatively small diameters (1.25 mm < dp < 2.50 mm) had the lowest impact. Smaller particles blend in a better manner with the remaining mix constituents creating a more homogenous mix in comparison to large particles. Test observations indicated that the latter are more dispersed and have a higher surface area which produces a less homogenous mix.

The flexural strength of a fibre-reinforced mortar is highly dependent on the embedment length and the aspect ratio of the fibre [62]. This would also be the case for an RPVC fibre/granule - mortar matrix. A relatively large amount of free water around the RPVC granules, which increases proportionally with the replacement ratio, results in a larger porosity and poorer adhesion [60]. Test observations from this paper and available literature showed that plastic granules could be removed manually from the matrix [63]. This effect was proportional with the embedment length of the particle. For fibres, as shown in Figure 2d, which due to their aspect ratio have a relatively longer embedment length and provide enhanced bond than the granules in Figure 2a,b,c, the post-peak

enhancement was significantly higher. This agrees with other studies in the literature that suggest that the ductility enhancement with an increase in replacement ratio, is due to the elongated structure of the PVC aggregates which helps delay the separation of PVC particles and the surrounding matrix [61].

5. Conclusions

This paper described an experimental investigation into the fundamental mechanical properties of cementitious composites incorporating granules and fibres from recycled Reinforced PVC (RPVC) banners. A detailed account of over 140 tests on cylindrical, cubic and prismatic specimens tested in compression and flexure, was given. In addition, a detailed assessment of the uniaxial properties of selected recycled materials, as well as characterisation of the RPVC granule size and geometry, was presented. Detailed measurements using digital image correlation techniques enabled assessment of the full constitutive response in compression, depiction of the flexural stress-crack opening curves, as well as determination of the key mechanical parameters, including the strength, elastic modulus and fracture energy of the investigated RPVC composites. The key findings are outlined below.

The test results showed that the compressive strength decreased proportionally with the amount of RPVC. For each 10% incremental increase in the volumetric replacement of mineral aggregates, the compressive strength was halved. The compressive strength of elements with 10% replacement was shown to be in the range of 32-47% of its reference value, depending on the RPVC particle size, whilst for 20% replacement, this was less than a quarter of the conventional material. The reduction in strength was counterbalanced by an enhanced ductility, represented by a softer and more ductile post-peak response, which is attributed to the crack-bridging effect of RPVC granules and fibres. It was also shown that the plastic particles enhanced the crushing energy by a factor of 2.6-3.5, depending on the particle size. Smaller particle sizes had less impact on the degradation of elastic and compressive strength properties of RPVC cementitious composites but provided lower levels of energy absorption.

It was shown that specimens incorporating RPVC granules exhibited residual flexural strength and enhanced softening proportional to the increase in replacement ratio. For a 20% replacement, the flexural strength reduction ratio was between 0.52 and 0.63, which was less than that in compression. The enhanced post-peak softening observed in flexural tests on both mortar and concrete, resulted from the clamping action produced by the RPVC particles that bridged the crack and limited the crack width opening. Smaller particles, which had a relatively long acicular or triangular geometry, provided a more favourable performance. These acted as fibres with a higher

relative embedment length, and hence improved the bond properties in comparison with intermediate and large size granules.

Importantly, the test results and observations enabled the definition of a series of expressions to determine the mechanical properties of cementitious materials incorporating RPVC and other waste plastics. These expressions were then used as a basis for developing and an analytical model for assessing the compressive and tensile stress-strain response of such materials. Validations carried out using the tests from this paper, as well as from a collated database, showed that the proposed expressions and the suggested constitutive model offer reliable representations that can be used in practical applications.

Acknowledgements: The support of Breedon Group, Elkem, Sika and Plas Cycle through the provision of materials is gratefully acknowledged.

Credit author statement: D.V. Bompa: *Conceptualization, Methodology, Investigation, Formal analysis, Writing - Original Draft;* B. Xu: *Conceptualization, Methodology, Investigation;* A.Y. Elghazouli: *Conceptualization, Resources, Writing - Review & Editing*

Conflict of interest: The authors declare that they have no conflict of interest.

References

[1] European Commission, 2018. A European strategy for plastics in a circular economy. Report COM(2018) 28 final. Brussels

[2] Geyer, R., Jambeck, J.R. and Law, K.L., 2017. Production, use, and fate of all plastics ever made. Science advances, 3(7), p.e1700782. https://dx.doi.org/10.1126/sciadv.1700782

[3] British Plastics Federation, 2019. VinylPlus UK. London

[4] Zhou, Y., Yang, N. and Hu, S., 2013. Industrial metabolism of PVC in China: A dynamic material flow analysis. Resources, Conservation and Recycling, 73, pp.33-40. https://doi.org/10.1016/j.resconrec.2012.12.016

[5] Keane, M.A., 2007. Catalytic conversion of waste plastics: focus on waste PVC. Journal of Chemical Technology & Biotechnology: International Research in Process, Environmental & Clean Technology, 82(9), pp.787-795. https://doi.org/10.1002/jctb.1757

[6] Kameda, T., Fukuda, Y., Grause, G. and Yoshioka, T., 2010. Chemical modification of rigid poly (vinyl chloride) by the substitution with nucleophiles. Journal of applied polymer science, 116(1), pp.36-44. https://doi.org/10.1002/app.31452

[7] Wu, C.H., Chang, C.Y., Hor, J.L., Shih, S.M., Chen, L.W. and Chang, F.W., 1994. Two-Stage pyrolysis model of PVC. The Canadian Journal of Chemical Engineering, 72(4), pp.644-650. https://doi.org/10.1002/cjce.5450720414

[8] Grigoryeva, O., Fainleib, A., Stepanenko, L., Sergeeva, L. and Pissis, P., 2005. Recycling of PVC/PU waste and reuse in PVC formulations: Structure-property relationship. Polymer Engineering & Science, 45(6), pp.801-808. https://doi.org/10.1002/pen.20343

[9] Cholake, S.T., Pahlevani, F., Gaikwad, V., Millicer, H. and Sahajwalla, V., 2018. Cost-effective and sustainable approach to transform end-of-life vinyl banner to value added product. Resources, Conservation and Recycling, 136, pp.9-21. https://doi.org/10.1016/j.resconrec.2018.03.025

[10] Saikia, N. and De Brito, J., 2012. Use of plastic waste as aggregate in cement mortar and concrete preparation: A review. Construction and Building Materials, 34, pp.385-401. https://doi.org/10.1016/j.conbuildmat.2012.02.066

[11] Sharma, R. and Bansal, P.P., 2016. Use of different forms of waste plastic in concrete–a review. Journal of Cleaner Production, 112, pp.473-482. https://doi.org/10.1016/j.jclepro.2015.08.042

[12] Bompa, D.V., Elghazouli, A.Y., Xu, B., Stafford, P.J. and Ruiz-Teran, A.M., 2017. Experimental assessment and constitutive modelling of rubberised concrete materials. Construction and Building Materials, 137, pp.246-260. https://doi.org/10.1016/j.conbuildmat.2017.01.086

[13] Sabau, M. and Vargas, J.R., 2018. Use of e-plastic waste in concrete as a partial replacement of coarse mineral aggregate. Computers and Concrete, 21(4), pp.377-384. https://doi.org/10.12989/cac.2018.21.4.377

[14] Spadea, S., Farina, I., Berardi, V.P., Dentale, F. and Fraternali, F., 2014. Energy dissipation capacity of concretes reinforced with recycled PET fibers. Ing. Sismica, 31(2), pp.61-70.

[15] Choi, Y.W., Moon, D.J., Kim, Y.J. and Lachemi, M., 2009. Characteristics of mortar and concrete containing fine aggregate manufactured from recycled waste polyethylene terephthalate bottles. Construction and Building Materials, 23(8), pp.2829-2835. https://doi.org/10.1016/j.conbuildmat.2009.02.036

[16] Nikbin, I.M., Rahimi, S., Allahyari, H. and Fallah, F., 2016. Feasibility study of waste Poly Ethylene Terephthalate (PET) particles as aggregate replacement for acid erosion of sustainable structural normal and lightweight concrete. Journal of Cleaner Production, 126, pp.108-117. https://doi.org/10.1016/j.jclepro.2016.02.143

[17] Sadrmomtazi, A., Dolati-Milehsara, S., Lotfi-Omran, O. and Sadeghi-Nik, A., 2016. The combined effects of waste Polyethylene Terephthalate (PET) particles and pozzolanic materials on the properties of self-compacting concrete. Journal of Cleaner Production, 112, pp.2363-2373. https://doi.org/10.1016/j.jclepro.2015.09.107

[18] Pereira, E.L. de Oliveira Junior, A.L. and Fineza, A.G., 2017. Optimization of mechanical properties in concrete reinforced with fibers from solid urban wastes (PET bottles) for the production of ecological concrete. Construction and Building Materials, 149, pp.837-848. https://doi.org/10.1016/j.conbuildmat.2017.05.148

[19] Pešić, N., Živanović, S., Garcia, R. and Papastergiou, P., 2016. Mechanical properties of concrete reinforced with recycled HDPE plastic fibres. Construction and Building Materials, 115, pp.362-370. https://doi.org/10.1016/j.conbuildmat.2016.04.050

[20] Bhavi, B.K., Reddy, V.V. and Ullagaddi, P.B., 2012. Effect of Different Percentages of Waste High Density Polyethylene (HDPE) Fibres on the Properties of Fibre Reinforced Concrete. Nature Environment and Pollution Technology, 11(3), p.461.

[21] Alhozaimy, A.M. and Shannag, M.J., 2009. Performance of concretes reinforced with recycled plastic fibres. Magazine of Concrete Research, 61(4), pp.293-298. https://doi.org/10.1680/macr.2008.00053

[22] Guendouz, M., Debieb, F., Boukendakdji, O., Kadri, E.H., Bentchikou, M. and Soualhi, H., 2016. Use of plastic waste in sand concrete. J. Mater. Environ. Sci, 7(2), pp.382-389.

[23] Kou, S.C., Lee, G., Poon, C.S. and Lai, W.L., 2009. Properties of lightweight aggregate concrete prepared with PVC granules derived from scraped PVC pipes. Waste Management, 29(2), pp.621-628. https://doi.org/10.1016/j.wasman.2008.06.014

[24] Kurup, A.R. and Senthil Kumar, K., 2017. Effect of recycled PVC fibers from electronic waste and silica powder on shear strength of concrete. Journal of Hazardous, Toxic, and Radioactive Waste, 21(3), p.06017001. https://doi.org/10.1061/(ASCE)HZ.2153-5515.0000354

[25] Mohammadhosseini, H., Abdul Awal, A. and Mohd Yatim, J.B., 2017. The impact resistance and mechanical properties of concrete reinforced with waste polypropylene carpet fibres. Construction and Building Materials, 143, pp.147-157. https://doi.org/10.1016/j.conbuildmat.2017.03.109

[26] Yin, S., Tuladhar, R., Collister, T., Combe, M., Sivakugan, N. and Deng, Z., 2015. Post-cracking performance of recycled polypropylene fibre in concrete. Construction and Building Materials, 101, pp.1069-1077. https://doi.org/10.1016/j.conbuildmat.2015.10.056

[27] Rubio-de Hita, P., Pérez-Gálvez, F., Morales-Conde, M.J. and Pedreño-Rojas, M.A., 2018. Reuse of plastic waste of mixed polypropylene as aggregate in mortars for the manufacture of pieces for restoring jack arch floors with timber beams. Journal of Cleaner Production, 198, pp.1515-1525. https://doi.org/10.1016/j.jclepro.2018.07.065

[28] Tang, W.C., Cui, H.Z. and Wu, M., 2014. Creep and creep recovery properties of polystyrene aggregate concrete. Construction and Building Materials, 51, pp.338-343. https://doi.org/10.1016/j.conbuildmat.2013.10.093

[29] Mondal, M.K., Bose, B.P. and Bansal, P., 2019. Recycling waste thermoplastic for energy efficient construction materials: An experimental investigation. Journal of Environmental Management, 240, pp.119-125. https://doi.org/10.1016/j.jenvman.2019.03.016

[30] Mohammed, A.A., 2017. Modelling the mechanical properties of concrete containing PET waste aggregate. Construction and Building Materials, 150, pp.595-605. https://doi.org/10.1016/j.conbuildmat.2017.05.154

[31] CEN (European Committee for Standardization) EN 933-1:2012 Tests for geometrical properties of aggregates – Part 1: Determination of particle size distribution – Sieving method. CEN, Brussels (Belgium); 2012

[32] Rabbani, A., Ayatollahi, S., 2015. Comparing three image processing algorithms to estimate the grain-size distribution of porous rocks from binary 2d images and sensitivity analysis of the grain overlapping degree. Special Topics & Reviews in Porous Media: An International Journal 6 (1), 71-89.

[33] CEN (European Committee for Standardization) EN 197-1:2011 Cement. Composition, specifications and conformity criteria for common cements, CEN, Brussels (Belgium); 2011

[34] CEN (European Committee for Standardization) EN 450-1:2012 Fly ash for concrete – Part 1. Definition, specifications and conformity criteria, CEN, Brussels (Belgium); 2012

[35] CEN (European Committee for Standardization) EN 1015-2: Methods of test for mortar for masonry-Part 2: Bulk sampling of mortars and preparation of test mortars. CEN, Brussels (Belgium); 1999

[36] LaVision - DaVis digital image correlation software http://www.lavision.de/en/products/davis-software/index.php [accessed 10 November 2019]

[37] Kim, S.B., Yi, N.H., Kim, H.Y., Kim, J.H.J. and Song, Y.C., 2010. Material and structural performance evaluation of recycled PET fiber reinforced concrete. Cement and concrete composites, 32(3), pp.232-240. https://doi.org/10.1016/j.cemconcomp.2009.11.002

[38] Merli, R., Preziosi, M., Acampora, A., Lucchetti, M.C. and Petrucci, E., 2019. Recycled Fibers in Reinforced Concrete: a systematic literature review. Journal of Cleaner Production, p.119207. https://doi.org/10.1016/j.jclepro.2019.119207

[39] Ramezanianpour, A.A., Esmaeili, M., Ghahari, S.A. and Najafi, M.H., 2013. Laboratory study on the effect of polypropylene fiber on durability, and physical and mechanical characteristic of concrete for application in sleepers. Construction and Building Materials, 44, pp.411-418. https://doi.org/10.1016/j.conbuildmat.2013.02.076

[40] de la Fuente, A., Escariz, R.C., de Figueiredo, A.D. and Aguado, A., 2013. Design of macro-synthetic fibre reinforced concrete pipes. Construction and Building Materials, 43, pp.523-532. https://doi.org/10.1016/j.conbuildmat.2013.02.036

[41] Ismail, Z.Z. and Al-Hashmi, E.A., 2008. Use of waste plastic in concrete mixture as aggregate replacement. Waste management, 28(11), pp.2041-2047. https://doi.org/10.1016/j.wasman.2007.08.023

[42] Batayneh, M., Marie, I. and Asi, I., 2007. Use of selected waste materials in concrete mixes. Waste management, 27(12), pp.1870-1876. https://doi.org/10.1016/j.wasman.2006.07.026

[43] Rahmani, E., Dehestani, M., Beygi, M.H.A., Allahyari, H. and Nikbin, I.M., 2013. On the mechanical properties of concrete containing waste PET particles. Construction and Building Materials, 47, pp.1302-1308. https://doi.org/10.1016/j.conbuildmat.2013.06.041

[44] Almeshal, I., Tayeh, B.A., Alyousef, R., Alabduljabbar, H. and Mohamed, A.M., 2020. Eco-friendly concrete containing recycled plastic as partial replacement for sand. Journal of Materials Research and Technology. https://doi.org/10.1016/j.jmrt.2020.02.090

[45] Hannawi, K., Kamali-Bernard, S. and Prince, W., 2010. Physical and mechanical properties of mortars containing PET and PC waste aggregates. Waste management, 30(11), pp.2312-2320. https://doi.org/10.1016/j.wasman.2010.03.028

[46] Saikia, N. and de Brito, J., 2014. Mechanical properties and abrasion behaviour of concrete containing shredded PET bottle waste as a partial substitution of natural aggregate. Construction and Building Materials, 52, pp.236-244. https://doi.org/10.1016/j.conbuildmat.2013.11.049

[47] Olofinnade, O., Chandra, S. and Chakraborty, P., 2020. Recycling of high impact polystyrene and low-density polyethylene plastic wastes in lightweight based concrete for sustainable construction. Materials Today: Proceedings. https://doi.org/10.1016/j.matpr.2020.05.176

[48] Zéhil, G.P. and Assaad, J.J., 2019. Feasibility of concrete mixtures containing cross-linked polyethylene waste materials. Construction and Building Materials, 226, pp.1-10. https://doi.org/10.1016/j.conbuildmat.2019.07.285

[49] CEN (European Committee for Standardization). EN 1992-1-1, Eurocode 2: Design of concrete structures, Part 1–1: General rules for buildings. CEN, Brussels (Belgium); 2004

[50] Neville AM. The relation between standard deviation and mean strength of concrete test cubes. Magazine of Concrete Research 1959;11(32):75-84 https://doi.org/10.1680/macr.1959.11.32.75

[51] Himsworth FR. The variability of concrete and its effect on mix design. Proceedings of the Institution of Civil Engineers 1945;3(2):163-200 https://doi.org/10.1680/iicep.1954.11167

[52] fib Model Code 2010. fib bulletins 65 and 66. fib, Lausanne (Switzerland); 2012

[53] Reinhardt H, Cornelissen H, Hordijk D. Tensile Tests and Failure Analysis of Concrete. J. Struct. Eng. 1986;112(11):2462-2477.

[54] Xu, X., Zhang, Z., Hu, Y. and Wang, X., 2020. Bearing Strength of Crumb Rubber Concrete under Partial Area Loading. Materials, 13(11), p.2446. https://doi.org/10.3390/ma13112446

[55] Khusru, S., Fawzia, S., Thambiratnam, D.P. and Elchalakani, M., 2020. A parametric study: High performance double skin tubular column using rubberised concrete. Composite Structures, 235, p.111741. https://doi.org/10.1016/j.compstruct.2019.111741

[56] Xu, B., Bompa, D.V., Elghazouli, A.Y., Ruiz-Teran, A.M. and Stafford, P.J., 2020. Numerical assessment of reinforced concrete members incorporating recycled rubber materials. Engineering Structures, 204, p.110017. https://doi.org/10.1016/j.engstruct.2019.110017

[57] Wang, Z., Hu, H., Hajirasouliha, I., Guadagnini, M. and Pilakoutas, K., 2020. Tensile stress-strain characteristics of rubberised concrete from flexural tests. Construction and Building Materials, 236, p.117591. https://doi.org/10.1016/j.conbuildmat.2019.117591

[58] Kaur, G. and Pavia, S., 2020. Physical properties and microstructure of plastic aggregate mortars made with acrylonitrile-butadiene-styrene (ABS), polycarbonate (PC), polyoxymethylene (POM) and ABS/PC blend waste. Journal of Building Engineering, p.101341. https://doi.org/10.1016/j.jobe.2020.101341

[59] Choi, Y.W., Moon, D.J., Kim, Y.J. and Lachemi, M., 2009. Characteristics of mortar and concrete containing fine aggregate manufactured from recycled waste polyethylene terephthalate bottles. Construction and Building Materials, 23(8), pp.2829-2835. https://doi.org/10.1016/j.conbuildmat.2009.02.036

[60] Yang, S., Yue, X., Liu, X. and Tong, Y., 2015. Properties of self-compacting lightweight concrete containing recycled plastic particles. Construction and Building Materials, 84, pp.444-453. http://dx.doi.org/10.1016/j.conbuildmat.2015.03.038

[61] Senhadji, Y., Siad, H., Escadeillas, G., Benosman, A.S., Chihaoui, R., Mouli, M. and Lachemi, M., 2019. Physical, mechanical and thermal properties of lightweight composite mortars containing recycled polyvinyl chloride. Construction and Building Materials, 195, pp.198-207. https://doi.org/10.1016/j.conbuildmat.2018.11.070

[62] Ţibea, C. and Bompa, D.V., 2020. Ultimate shear response of ultra-high-performance steel fibre-reinforced concrete elements. Archives of Civil and Mechanical Engineering, 20, pp.1-16. https://doi.org/10.1007/s43452-020-00051-z

[63] Hannawi, K., Kamali-Bernard, S. and Prince, W., 2010. Physical and mechanical properties of mortars containing PET and PC waste aggregates. Waste management, 30(11), pp.2312-2320. http://doi.org/10.1016/j.wasman.2010.03.028